Biochimica et Biophysica Acta 1840 (2014) 1798–1807

Contents lists available at ScienceDirect

Biochimica et Biophysica Acta

journal homepage: www.elsevier.com/locate/bbagen

Subunit interactions in pig-kidney fructose-1,6-bisphosphatase: Binding of substrate induces a second class of site with lowered affinity and catalytic activity

Joel L. Asenjo [a], Heide C. Ludwig [a], Cristian A. Droppelmann [a,1], Juan G. Cárcamo [a], Ilona I. Concha [a], Alejandro J. Yáñez [a], María L. Cárdenas [b], Athel Cornish-Bowden [b], Juan C. Slebe [a,*]

[a] Instituto de Bioquímica y Microbiología, Facultad de Ciencias, Universidad Austral de Chile, Valdivia, Chile
[b] Bioénergétique et Ingénierie des Protéines, Institut de Microbiologie de la Méditerranée, CNRS, Aix-Marseille Université, Marseilles, France

ARTICLE INFO

Article history:
Received 23 July 2013
Received in revised form 28 November 2013
Accepted 23 December 2013
Available online 18 January 2014

Keywords:
FBPase
Gluconeogenesis
Substrate inhibition
Fructose-1,6-bisphosphate
Affinity site
Subunit interaction

ABSTRACT

Background: Fructose-1,6-bisphosphatase, a major enzyme of gluconeogenesis, is inhibited by AMP, Fru-2,6-P_2 and by high concentrations of its substrate Fru-1,6-P_2. The mechanism that produces substrate inhibition continues to be obscure.
Methods: Four types of experiments were used to shed light on this: (1) kinetic measurements over a very wide range of substrate concentrations, subjected to detailed statistical analysis; (2) fluorescence studies of mutants in which phenylalanine residues were replaced by tryptophan; (3) effect of Fru-2,6-P_2 and Fru-1,6-P_2 on the exchange of subunits between wild-type and Glu-tagged oligomers; and (4) kinetic studies of hybrid forms of the enzyme containing subunits mutated at the active site residue tyrosine-244.
Results: The kinetic experiments with the wild-type enzyme indicate that the binding of Fru-1,6-P_2 induces the appearance of catalytic sites with lower affinity for substrate and lower catalytic activity. Binding of substrate to the high-affinity sites, but not to the low-affinity sites, enhances the fluorescence emission of the Phe219Trp mutant; the inhibitor, Fru-2,6-P_2, competes with the substrate for the high-affinity sites. Binding of substrate to the low-affinity sites acts as a "stapler" that prevents dissociation of the tetramer and hence exchange of subunits, and results in substrate inhibition.
Conclusions: Binding of the first substrate molecule, in one dimer of the enzyme, produces a conformational change at the other dimer, reducing the substrate affinity and catalytic activity of its subunits.
General significance: Mimics of the substrate inhibition of fructose-1,6-bisphosphatase may provide a future option for combatting both postprandial and fasting hyperglycemia.

1. Introduction

The two irreversible reactions that interconvert Fru-6-*P* and Fru-1,6-P_2 constitute a major crossroads of metabolism. Phosphorylation of Fru-6-*P* is catalyzed by PFK, and hydrolysis of Fru-1,6-P_2 is catalyzed by FBPase [1]. Both enzymes are regulated by Fru-1,6-P_2 (product activation for PFK, substrate inhibition for FBPase) and by a series of effectors, of which we shall be concerned with AMP and Fru-2,6-P_2 [1–7] in this paper (Fig. 1). The opposite effects of AMP and Fru-2,6-P_2 on the two enzymes are readily rationalized, as both act as signals of ATP concentration, stimulating glycolysis when this is low, and simultaneously inhibiting gluconeogenesis. However, there is another symmetry in Fig. 1 that is more surprising: both enzymes are subject to inhibition by excess of substrate, PFK by ATP, and FBPase by Fru-1,6-P_2. For PFK this is to be expected, because although ATP is a substrate it is also a major product of glycolysis, so the substrate inhibition can be regarded as a form of feedback inhibition. The superficially similar substrate inhibition of FBPase by Fru-1,6-P_2 is more puzzling, as there is no obvious physiological function.

The inhibition of FBPase by excess substrate has been known for many years [8], and two different hypotheses have been proposed, to explain it, on the one hand that it is strictly a kinetic process [9]; and on the other that it is due to allosteric substrate inhibition [10], though crystallographic studies of the enzyme–Fru-2,6-P_2 complex do not support the existence of an allosteric site [11]. The mechanism of inhibition of FBPase by Fru-2,6-P_2 involves binding of the two fructose bisphosphate molecules at the same site, albeit with different binding determinants [12]. The substrate inhibition of FBPase occurs at rather

Abbreviations: FBPase, fructose-1,6-bisphosphatase (D-fructose-1,6-bisphosphate 1-phosphohydrolase, EC 3.1.3.11); PFK, phosphofructokinase (ATP:D-fructose-6-phosphate 1-phosphotransferase, EC 2.7.1.11); Fru-1,6-*P*2, fructose 1,6-bisphosphate; Fru-2,6-*P*2, fructose 2,6-bisphosphate; Glu-tag, C-terminal extension of nine glutamate residues

* Corresponding author at: Instituto de Bioquímica y Microbiología, Facultad de Ciencias, Universidad Austral de Chile, Campus Isla Teja, Valdivia, Chile. Tel./fax: +56 63 221332.
E-mail address: jslebe@uach.cl (J.C. Slebe).
[1] Current Address: Robarts Research Institute, University of Western Ontario, London, Ontario, Canada.

0304-4165/$ – see front matter © 2013 Elsevier B.V. All rights reserved.
http://dx.doi.org/10.1016/j.bbagen.2013.12.027

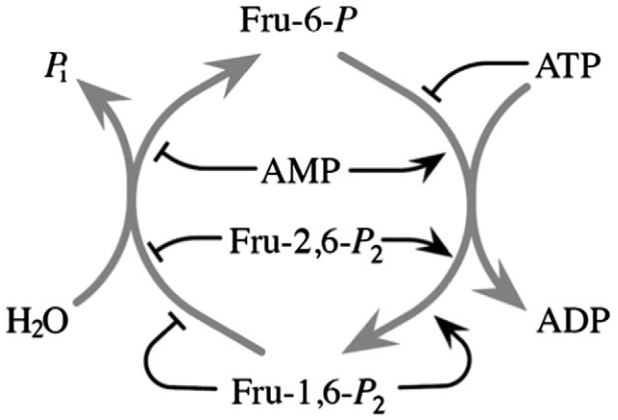

Fig. 1. Regulation of FBPase and phosphofructokinase. The two enzymes are regulated in opposite directions by AMP and Fru-2,6-P_2, and both are also inhibited by excess substrate, FBPase by Fru-1,6-P_2 and phosphofructokinase by ATP. Although the latter is well understood in terms of metabolic regulation, the role of the former remains unclear.

non-physiological concentrations of Fru-1,6-P_2, but its conservation in widely different organisms [2,13–19] suggests the existence of a function. Moreover, although inhibition by excess substrate is found in numerous enzymes with multiple substrates it is rare in one-substrate enzymes and hydrolases [20].

The general structure of pig-kidney FBPase is illustrated schematically in Fig. 2. It is a tetramer with D_2 symmetry with identical 37 kDa subunits designated C1, C2, C3 and C4, organized as a dimer of dimers C1C2 and C3C4 [21,22]. Each subunit has two folding domains, an AMP domain in residues 1–200 and a catalytic domain in residues 201–337. There are two quaternary structures, the R and the T states, with the R to T transition triggered by the binding of AMP to an allosteric site [21–24].

The mechanism of inhibition by Fru-1,6-P_2 needs to be understood, because the search for therapeutic inhibitors of FBPase is an active

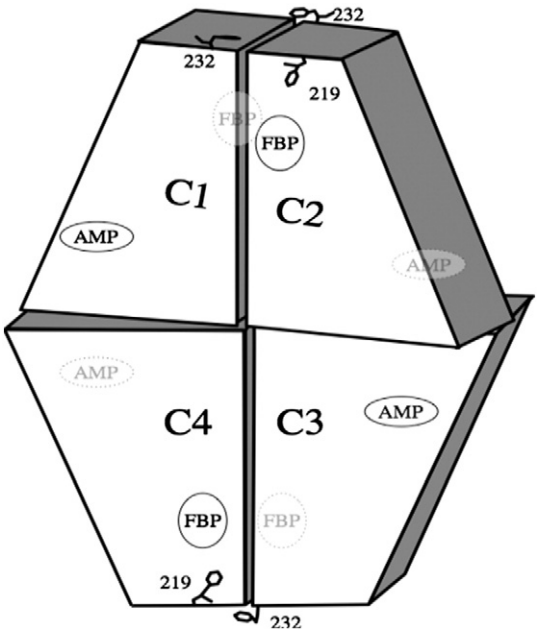

Fig. 2. Schematic drawing of FBPase. The active site, i.e. the site of binding Fru-1,6-P_2, is labeled FBP, and the AMP binding site is labeled AMP. Dotted ovals with gray labeling indicate the ligand binding sites on the faces of the tetramer that are hidden from view. The tetramer is shown in the T-state conformation. The location of residues 219 and 232 involved in the Phe219Trp and Phe232Trp mutants used in the fluorescence experiments are marked, together with diagrams indicating the Phe side chains schematically. The location of residue 244 involved in the Tyr244Phe mutant is not explicitly labeled as it is in the active site and thus in the same position as the FBP labels.

area of research [25–29], on account of the importance of gluconeogenesis in type 2 diabetes [30,31] and other serious illnesses. We have shown that nuclear accumulation of FBPase *in vivo* is impaired in diabetic rat liver [32] and this may be an important regulatory mechanism that could account for the increased gluconeogenic glucose production in the livers of diabetic rodents. Analogs of Fru-2,6-P_2 or Fru-1,6-P_2 are likely to be more suitable as drugs than analogs of AMP, because they can be expected to be more specific.

In this paper we shall present kinetic and fluorescence data, as well as studies of hybrid tetramers with mixed subunits, to clarify the cause of the inhibition.

2. Materials and methods

2.1. Biochemicals and chemicals

Fru-1,6-P_2, Fru-2,6-P_2, NAD^+, AMP, glucose-6-phosphate dehydrogenase and phosphoglucose isomerase were purchased from Sigma or Boehringer Mannheim and other chemicals came from Merck. All of them were of the highest available purity.

2.2. Site-directed mutagenesis

The Phe219Trp, Phe232Trp and Tyr244Phe FBPases were obtained using the Altered Sites II in vitro Mutagenesis Systems kit (Promega, Madison,WI), and the corresponding mutagenic oligonucleotides as previously described [22]. The following mutagenic oligonucleotide (with altered bases shown in bold) was used for mutation of Tyr in position 244: 5′-CCCTACGGGGCCAGG**TTC**GTGGGCTCCATGGTG-3′ (Tyr244Phe). Glu-tagged FBPase was obtained by adding nine Glu codons to the pig kidney cDNA by PCR. The oligonucleotide required as primer for the site-specific mutagenesis for Glu-tagged FBPase was 5′-TGGATCCTCA**TTCTTCTTCTTCTTCTTCTTCTTC**GCCTGCAGCCTTGGCT GCGTGCTTCTG-3′. The mutations were confirmed by sequencing. Protein expression and purification of Phe219Trp and Phe232Trp FBPases were performed as previously described [22]. For expression, the fragments encoding the wild-type, Glu-tagged FBPase and Tyr244Phe FBPase were excised from the corresponding plasmid and cloned into the vector pET22 (Novagen, San Diego, CA) as described [33]. The purification of Glu-tagged FBPase was performed by sequential chromatography on Cibacron Blue Sepharose CL-6B and DEAE-Sephacel. The purification of Tyr244Phe FBPase was made by sequential chromatography on Cibacron Blue Sepharose CL-6B and CM-Sepharose. Protein purity and concentration throughout the purification were monitored by SDS-PAGE and by Bio-Rad protein assay. The wild-type FBPase and the Phe219Trp, Phe232Trp and Tyr244Phe mutants, showed identical electrophoretic mobilities (37 kDa) whereas the FBPase mutant tagged with a 9-residue polyglutamyl extension at the C-terminal (Glu-tagged FBPase) shows an apparent mass of 38 kDa. All enzymes were >96% homogeneous using SDS-PAGE as a criterion (data not shown).

2.3. Activity assay

The spectrophotometric coupled enzyme assay was used to measure FBPase activity, as described previously [33]. Digital absorbance values were collected on a Hewlett Packard 8453 spectrophotometer and the data were fitted to a straight line on a coupled computer using the UV–visible Chem Station Program. Because FBPase exhibits substrate inhibition, the K_m and k_{cat} values were obtained by fitting the experimental data to a modified form of the Michaelis–Menten equation that incorporates a term for substrate inhibition [33,34]. The K_a value and Hill coefficient for Mg^{2+} were determined by fitting the saturation curves to the Hill equation. The inhibition curves elicited by AMP or Fru-2,6-P_2 were fitted to the equation of Taketa and Pogell [8].

2.4. Steady-state fluorescence measurements

Fluorescence data were collected using a Perkin Elmer Luminescence Spectrometer LS-50 equipped with a thermo-regulated stirred cell holder set at 15 ºC. This temperature was selected to prevent a possible denaturation of the mutant FBPases during the titration experiments. To avoid exciting tyrosyl side chains, an excitation wavelength of 295 nm was used. The excitation and emission slits were set to 7 nm. The enzymes were at a concentration of 60 μg/ml in 20 mM Tris/HCl buffer, pH 7.5, containing 0.1 mM EDTA. Ligands were tested to ensure that they do not influence the fluorescence emission of tryptophan. The maximum volume increase due to the sequential additions of ligand stock solutions was less than 5%. The emission spectrum was recorded one minute after addition of the ligand. Blanks were subtracted from all spectra, and corrections for protein dilutions were made. Fluorescence intensities were measured at the maximum of each spectrum. Data were fitted to the equation for a simple binding curve, $\Delta F/F_0 = \{(\Delta F/F_0)_{max}\, L\} / \{K_d + L\}$, where $\Delta F = F - F_0$, F is the observed fluorescence at a given concentration of ligand, F_0 is the fluorescence in the absence of ligand and L is the ligand concentration. For the titrations of the enzyme with substrate in the presence of Fru-2,6-P_2 $\Delta F = F - F_i$, where F_i is the fluorescence at the beginning of the titration (after the addition of Fru-2,6-P_2). Fluorescence quenching experiments were performed as previously described [22] using solutions of the enzymes in 20 mM Tris/HCl buffer, pH 7.5, containing 0.1 mM EDTA. Some experiments were done with Phe219Trp FBPase in the presence of 5 mM Mg^{2+} at 30 °C In these experiments a different enzyme sample was used for each substrate concentration. After the addition of substrate the fluorescence emission was recorded continuously over 3 min at the emission maximum of 335 nm. A constant intensity value was reached a few seconds (about 15 s) after the beginning of the fluorescence registration. Fluorescence intensities were measured after one minute and the data were treated as described for the experiments in the absence of Mg^{2+}.

2.5. Formation of hybrid enzymes

Solutions of pure wild-type FBPase and Glu-tagged FBPase in 20 mM Tris/HCl buffer, pH 7.5, containing 0.1 mM EDTA were mixed and incubated overnight at 4 °C in the absence or presence of Fru-1,6-P_2, Fru-2,6-P_2 or KCl at different concentrations. On the other hand, solutions of pure Tyr244Phe and Glu-tagged FBPases in 20 mM Tris/HCl buffer, pH 7.5, containing 0.1 mM EDTA were mixed and incubated

A

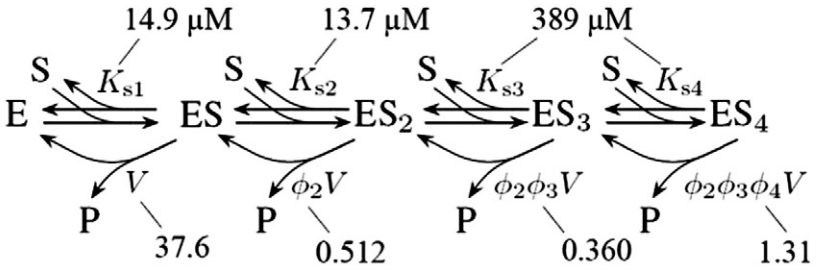

B

$$v = \frac{\frac{Vs}{K_{s1}}\left\{1 + \frac{\phi_2 s}{K_{s2}}\left[1 + \frac{\phi_3 s}{K_{s3}}\left(1 + \frac{\phi_4 s}{K_{s4}}\right)\right]\right\}}{1 + \frac{s}{K_{s1}}\left\{1 + \frac{s}{K_{s2}}\left[1 + \frac{s}{K_{s3}}\left(1 + \frac{s}{K_{s4}}\right)\right]\right\}} \qquad (1)$$

C

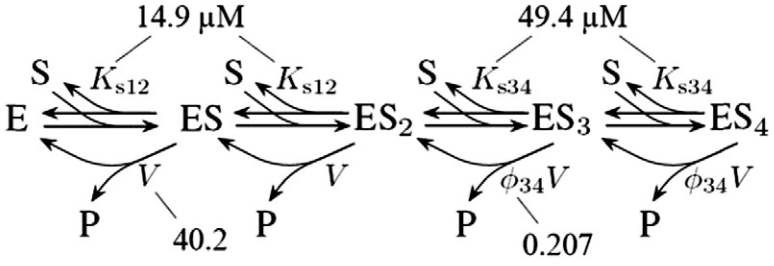

D

$$v = \frac{\frac{Vs}{K_{s12}}\left(1 + \frac{\phi_{34} s}{K_{s34}}\right)}{1 + \frac{s}{K_{s12}}\left(1 + \frac{s}{K_{s34}}\right)} \qquad (2)$$

Fig. 3. Scheme that illustrates two possible mechanisms for the inhibition of FBPase by Fru-1,6-P_2. A. Model with four non-independent sites, in which E is FBPase, S is the substrate Fru-1,6-P_2, and P is the product Fru-6-P. The numerical values shown (with V measured in μmol min^{-1} mg^{-1}) are the best-fit values obtained as described in the text. B. Eq. (1) shows the rate v for the model in A, in which s is the concentration of Fru-1,6-P_2, V is the limiting rate that would be observed if only the first site existed, K_{s1} … K_{s4} are the successive dissociation constants of the four sites, and φ_2 … φ_4 are the relative catalytic activities of the second, third and fourth sites with respect to the catalytic activities of the previous site. C. Model with two independent pairs of sites. D. Eq. (2) shows the rate for the model in C, in which the first and second sites have the same dissociation constant K_{s12} and the same limiting rate V, and the third and fourth sites have the same dissociation constant K_{s34} and φ_{34} is the relative catalytic activity of the third and fourth sites with respect to the catalytic activities of the first two.

overnight at 4 °C in the absence of ligands. The concentration of each enzyme in the mixture was 0.5 mg/ml.

2.6. Purification of enzymes with mixed Tyr244Phe and Glu-tagged subunits

The hybrid tetramers were purified by anion-exchange chromatography at room temperature, as described by Nelson et al. [35], except that a Q-Sepharose column coupled to an AKTAprime plus chromatographic system (Amersham) was used. Individual hybrids were eluted with 20 mM Tris/HCl, pH 7.5 and a linear gradient from 0.25 to 0.49 M NaCl in 20 mM Tris/HCl, pH 7.5. The identity and purity of the hybrid tetramers was checked by non-denaturing polyacrylamide gel electrophoresis. The purified hybrid enzymes were kept at room temperature since subunit exchange is slow at this temperature [35]: hybrid tetramers were stable for several hours at 25 °C, but not at 4 °C. All kinetic experiments were performed within 3 h of hybrid purification. After the activity measurements the integrity of the hybrids was rechecked.

2.7. Non-denaturing PAGE

This was done according to Laemmli [36], but omitting the SDS and β-mercaptoethanol from the loading and running buffers. The gels were stained and evaluated using GeneSnap 7.4 software (Syngene).

3. Results

3.1. Inhibition by excess Fru-1,6-P_2

FBPase has four binding sites for its substrate Fru-1,6-P_2, with marked substrate inhibition at Fru-1,6-P_2 concentrations over 20 μM. It has not been clear whether these binding sites have similar intrinsic affinity for the substrate, and whether they should be treated as four non-independent sites, or as two pairs of two sites with each pair of sites behaving independently of the other. The schemes shown in Fig. 3 illustrate the two possibilities. If the substrate binding sites are treated as four non-independent sites (Fig. 3A) the rate v should depend on Eq. (1) (Fig. 3B). However, if the four sites behave as two independent pairs (Fig. 3C) the equation is simpler, as given in Eq. (2) (Fig. 3D).

The numerous independent parameters of Eq. (1) demand a very careful and extensive kinetic study. We have made four experiments with essentially the same design, rates in each experiment being measured in triplicate for more than 40 Fru-1,6-P_2 concentrations in the range 0.5–5000 μM. All four experiments led to qualitatively very similar behavior, showing incomplete substrate inhibition in the limit at high concentrations (Fig. 4A).

Fitting the experimental data from one of these experiments (Fig. 4A) to Eq. (1) with eight independent parameters proved unsatisfactory, because there is not enough information in the data to define K_{s4} independently: essentially the same sum of squares can be obtained with any value of K_{s4} in a wide range: 0.267 for values of K_{s4} from 1 to 200 μM, increasing only to 0.279 at $K_{s4} = 10000$ μM. Accordingly we decreased the number of independent parameters from eight to seven by defining $K_{s4} \equiv K_{s3}$, an equivalence suggested by the similar values of K_{s1} and K_{s2} (Fig. 3A): if there is little difference in affinity between the first and second sites it is plausible to assume that there is little between the third and fourth.

3.2. Statistical analysis

Minimizing the weighted sum of squares $\Sigma(1 - v/v_{calc})^2$ for the two equations gave the parameter values shown next to the relevant parameters in Fig. 3A and C. Notice that this analysis indicates two sites of high affinity, and two of low affinity. The eight-fold decrease from $K_{s4} \equiv K_{s3} = 389$ μM in Eq. (1) to $K_{s34} = 49.4$ μM in Eq. (2) may appear surprising, but it probably reflects the need for stronger binding in the second model to compensate for the larger decrease in relative catalytic activity.

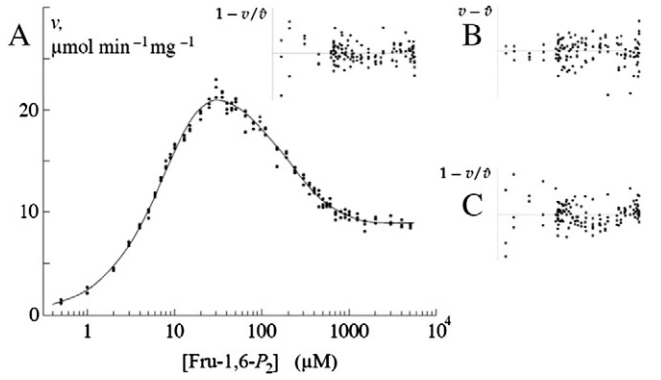

Fig. 4. Least-squares fit of data for FBPase measured at 44 concentrations of Fru-1,6-P_2, ranging from 0.5 μM to 5 mM. The assays were performed in 50 mM Tris/HCl (pH 7.5) at 5 mM Mg^{+2} and 30 °C as described in Materials and methods. A: Plot of v against log [Fru-1,6-P_2 (μM)], with a curve for v_{calc} calculated from Eq. (1) with the parameter values listed in Table 1, obtained by minimizing $\Sigma(1 - v/v_{calc})^2$. The corresponding residual plot of $1 - v/v_{calc}$ against v_{calc} is shown as an inset, without labeling, to avoid distracting attention away from the points: the abscissa axis ranges from 0 to 21, and the ordinate axis from −0.2 to +0.2. B: Residual plot of $v - v_{calc}$ against v_{calc} when the calculation was done by minimizing $\Sigma(v - v_{calc})^2$. Notice the approximately proportional increase in scatter as v_{calc} increases. The ordinate axis ranges from $v - v_{calc} = -2$ to $v - v_{calc} = 2$. C: Residual plot of $1 - v/v_{calc}$ against v_{calc} for data fitted to Eq. (2) with the same assumptions as for the main plot. The ordinate scale ranges from −0.2 to +0.2.

The two equations predict very similar properties with these parameter values, but with careful tests they can be distinguished. Fig. 4A shows the result of fitting the observations to Eq. (1), with each measured rate v assigned a weight $1/v_{calc}^2$, where v_{calc} is the calculated rate. This effectively assumes that the measured values have a uniform coefficient of variation, so that values of $1 - v/v_{calc}$ should show only random scatter. In fact the residuals plotted in the inset show a slight tendency to increase at low v_{calc}, but there are very few points in this region, and over most of the range the scatter is essentially random. If the calculation is repeated assigning equal weight to each v value, the residuals, illustrated in Fig. 4B, show a clear tendency to increase with v_{calc}, confirming that the standard deviation is not uniform. The real error behavior may be intermediate between these extremes, approximately proportional to v_{calc} when v_{calc} is large but remaining greater than zero when v_{calc} approaches zero [37,38].

When the data are fitted to Eq. (2) with weights $1/v_{calc}^2$ the residual plot (Fig. 4C) shows a weak suggestion of systematic error (a U-shaped pattern of residuals in the middle range) that is much less visible (though still possibly present) in the inset to Fig. 4A. Thus the data appear to fit Eq. (1) better than Eq. (2). However, the difference is sufficiently slight to require formal tests of significance.

The use of F tests for testing lack of fit is described by Draper and Smith [39] and in a more biochemical context by Cornish-Bowden [38]. The replicate observations allow assessment of the reproducibility independent of any fitted model ("pure error"), and this estimate allows the raw scatter of observations about a fitted line to be corrected to give a measure of lack of fit. Both of the resulting sums of squares can be converted to mean squares by dividing by the appropriate numbers of degrees of freedom (essentially the number of observations corrected by subtracting the number of degrees of freedom used for making the calculation). The ratio of these mean squares is Fisher's F, and its significance can be tested with standard tables [39].

Results for the FBPase data are given in Table 1. The first test shows that lack of fit to Eq. (2) is highly significant ($p < 0.01$): the value of F at the 1% level of significance for 40 and 88 degrees of freedom is not included as such in standard tables, but it must be less than 1.84, so the value of 2.57 found in the first test is highly significant: in other words lack of fit to Eq. (2) is highly significant. The second test shows that lack of fit to Eq. (1) is also significant, though at a less stringent level

Table 1
Tests for lack of fit.

Source of variation	Sum of squares	Degrees of freedom	Mean square	*F*
Testing lack of fit to Eq. (2)				
Total (corrected for V, K_{s12}, K_{s34}, φ_{34})	0.348016	128	0.00271887	
Lack of fit	0.187636	40	0.00469090	*2.5739***
Pure error	0.160380	88	0.00182250	
Testing lack of fit to Eq. (1)				
Total (corrected for V, K_{s1}…K_{s4}, φ_2…φ_4)	0.271324	125	0.00217059	
Lack of fit	0.110689	37	0.00299158	*1.6415**
Pure error	0.160380	88	0.00182250	
Testing significance of additional parameters in Eq. (2)				
Lack of fit for 4 parameters	0.187636	40	0.00469090	
K_{s2}, φ_2, φ_4/V, K_{s12}, K_{s34}; φ_{34}	0.076947	3	0.02564909	*8.5737***
Lack of fit for 7 parameters	0.110689	37	0.00299158	

** Highly significant ($p < 0.01$).
* Significant ($p < 0.05$).

($p < 0.05$). The third test confirms that passing from Eq. (2) to Eq. (1) results in a highly significant improvement. So there are arguments for rejecting the model expressed by Eq. (2), though it does give an approximate account of the data.

Figs. 3 and 4 and Table 1 indicate that the inhibition by Fru-1,6-P_2 is best explained in terms of two types of catalytic sites that differ in their affinity for the substrate, and the appearance of the low-affinity sites is induced by the binding of Fru-1,6-P_2, bringing about a decrease in the catalytic constants. Several questions then arise: (i) Does the inhibition by Fru-2,6-P_2 occur in a similar way, with Fru-2,6-P_2 binding to both types of sites, or only to one type? (ii) As the low-affinity sites are induced by the binding of Fru-1,6-P_2, implying strong subunit interactions, are these sites in the same dimer? (iii) If they are in different dimers, what are the geometrical relationships? Fluorescence measurements of mutant enzymes, together with studies of hybrid tetramers with mixed subunits, will be used to study these questions, and to compare the changes induced by the substrate and by Fru-2,6-P_2 and AMP.

3.3. Fluorescence measurements

Native pig-kidney FBPase contains no tryptophan, but it can be made fluorescent by mutating suitable residues, and we have studied two mutants, Phe219Trp, in the Fru-1,6-P_2 folding domain, close to the active site, and Phe232Trp, close to the C1–C2 interface (see Fig. 2). As previously reported [22] the kinetic parameters of these mutants, including those related to the interaction with Mg^{2+} and with the inhibitors AMP and Fru-2,6-P_2, are similar to those for recombinant wild-type and non-recombinant FBPases [22,33,35,40], and they also showed the characteristic partial inhibition by excess Fru-1,6-P_2 (data not shown). In agreement with the crystallographic structures of different enzyme–ligand complexes [11,41–43], the emission maxima of the mutants (Table 2) indicate that residue 219 is in a non-polar environment, whereas residue 232 is in a polar environment, exposed to the solvent [44].

Binding of the substrate Fru-1,6-P_2 or the inhibitors Fru-2,6-P_2 and AMP had different effects on the fluorescence emission intensities of the mutant enzymes (Fig. 5). These fluorescence changes reflect ligand-induced conformational changes indicative of ligand binding, as the ligands do not affect the fluorescence emission of a 1.64 μM *N*-acetyl-L-tryptophanamide solution (data not shown). Notice that in these conditions there is no product present, as the Fru-1,6-P_2 binding experiments were made in the absence of bivalent cations and so there was no enzyme-catalyzed hydrolysis. At concentrations near the K_m value of 6 μM [22], the substrate Fru-1,6-P_2 caused a 15% increase in the intrinsic fluorescence of the Phe219Trp enzyme (Fig. 5A). The transition was well described by a single binding isotherm (see Materials and methods), with a dissociation constant of 7.9 ± 1.3 μM. On the other hand, the fluorescence emission of the Phe232Trp mutant was not altered significantly by the substrate (Fig. 5A). Fig. 5B shows the corresponding effect of the inhibitor Fru-2,6-P_2: it caused a similar but much smaller increase (7%) of the intrinsic fluorescence of the Phe219Trp enzyme, with a dissociation constant of 1.3 ± 0.3 μM, but almost no perturbation of the Phe232Trp enzyme. Although there is a major change in the quaternary structure of the enzyme when the allosteric inhibitor AMP binds [21,24], AMP did not significantly affect the fluorescence of the enzymes (Fig. 5C). On the other hand, the degree of solvent accessibility for Trp 219 was somewhat reduced by binding of AMP and Fru-2,6-P_2, but not by substrate binding, as measured by the Stern–Volmer constant for acrylamide. The accessibility of Trp232 was not decreased by these ligands (Table 2).

The effect of Fru-1,6-P_2 on the fluorescence emission appears to be due to the binding to the high-affinity sites predicted by the analysis of the kinetic experiments, as it is observed at rather low substrate concentrations; in addition Fru-2,6-P_2 and Fru-1,6-P_2 do not produce the same conformational change, although most probably they bind to the same site but using different determinants [12]. This point was further explored by studying the effect of Fru-2,6-P_2 on substrate binding by means of measurements of the intrinsic fluorescence changes of the Phe219Trp enzyme generated by the substrate in presence of two different inhibitory concentrations of Fru-2,6-P_2 (Fig. 6). As expected for competitive binding, the affinity for the substrate is decreased by the inhibitor, and the dissociation constants increase: 15.1 ± 1.0 μM at 1.5 μM Fru-2,6-P_2, and 27.8 ± 3.4 μM at 5 μM Fru-2,6-P_2. However, the data indicate that the inhibitor is not completely displaced by the substrate, supporting the idea that different binding determinants are involved.

Table 2
Effect of ligands on the Stern–Volmer quenching constants and the fluorescence emission maxima of the FBPase tryptophan mutants.

Ligand	None		AMP (20 μM)		Fru-1,6-P_2 (150 μM)		Fru-2,6-P_2 (50 μM)	
	K_{SV} (M^{-1})	λ_{max} (nm)	K_{SV} (M^{-1})	λ_{max} (nm)	K_{SV} (M^{-1})	λ_{max} (nm)	K_{SV} (M^{-1})	λ_{max} (nm)
Phe219Trp	3.19 ± 0.12	335	2.89 ± 0.04	336	3.20 ± 0.10	335	2.78 ± 0.11	336
Phe232Trp	11.6 ± 0.3	352	11.7 ± 0.2	352	11.3 ± 0.3	354	11.4 ± 0.2	354

K_{SV}: Stern–Volmer quenching constant for acrylamide.

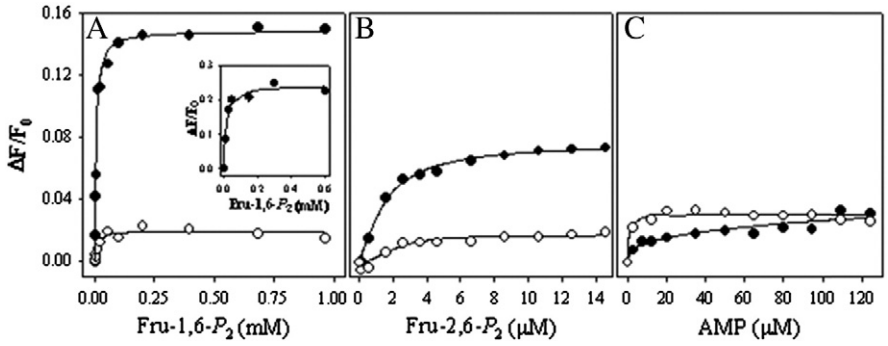

Fig. 5. Effect of substrate, Fru-2,6-P_2 or AMP on the fluorescence emission of FBPase mutants. Samples of Phe219Trp FBPase (●) or Phe232Trp FBPase (○) at a concentration of 60 μg/ml in Tris/HCl pH 7.5 containing 0.1 mM EDTA were titrated with solutions of the ligands and the fluorescence intensity at the maximum of the corresponding emission spectrum was measured upon excitation at 295 nm. The inset to Panel A shows $\Delta F/F_0$ obtained by the addition of substrate to samples of Phe219Trp FBPase containing 5 mM Mg^{2+} at 30 ºC, as described in Material and methods. The data were fitted to a simple binding curve after correction for buffer emission and protein dilution.

In addition to the results obtained in the absence of added Mg^{2+}, we also carried out experiments with the Phe219Trp FBPase and Fru-1,6-P_2 at 5 mM Mg^{2+}. In these experiments substrate at various concentrations was added to different enzyme/Mg^{2+} samples and the fluorescence emission was recorded continuously over 3 min. The results (illustrated in the inset to Fig. 5A) were essentially identical to those obtained in the absence of Mg^{2+} (Fig. 5A) but with a slightly higher (23%) increase in fluorescence. It was shown [45,46] that the binding of the substrate and divalent metal ions to FBPase is ordered; since a structural metal ion must be bound prior to substrate in order for catalysis to be functional. It appears that the role of the metal ion is to adapt the active site for maximum catalytic efficiency [45]. Benkovic's group has also reported [46] that Fru-1,6-P_2 binds to the rabbit liver enzyme in the absence of added metal ion. However, they suggested that this interaction probably reflects binding of substrate to FBPase containing at least two tightly bound structural metal ions (Zn^{2+}/Mn^{2+}) per molecule. Although the fluorescence experiments in the absence of Mg^{2+} were performed in the presence of 0.1 mM EDTA, we cannot rule out the possibility that the enzyme had contained Zn^{2+} as structural metal ion as a result of contamination.

3.4. Hybrid tetramers with mixed subunits

Hybrid enzymes with mixed subunits offer a powerful approach to the study of enzyme structure and function, and were used very effectively by Nelson et al. [35] for studying inhibition of FBPase by AMP. They did not study Fru-1,6-P_2 inhibition, but essentially the same strategy can be used, as we have done to shed light on the conformational changes induced by Fru-1,6-P_2 and Fru-2,6-P_2. Two types of hybrids have been used (i) hybrids between the wild type enzyme and a Glu-tagged enzyme, and (ii) hybrids between Tyr244Phe FBPase and the Glu-tagged wild-type enzyme.

3.5. Effects of Fru-1,6-P_2 and Fru-2,6-P_2 on subunit exchange

To compare the interaction of Fru-1,6-P_2 and Fru-2,6-P_2 with FBPase, we studied the effects of these ligands on the subunit exchange between wild-type and Glu-tagged enzyme. The hybrid mixtures obtained after incubation overnight were analyzed by non-denaturing gel electrophoresis. As expected, there were five bands, representing ratios of wild-type to Glu-tagged subunits of 4:0, 3:1, 2:2, 1:3 and 0:4 (Fig. 7, lanes 1A, 1B, 1C), in the absence of any added ligands. The most intense hybrid band corresponds to the 2:2 subunit ratios, whereas the band for the 3:1 and 1:3 hybrids were weak. At time zero there were only two bands, corresponding to the wild-type and Glu-tagged tetramers (not shown). Increasing concentrations of Fru-1,6-P_2 prevent the subunit exchange, indicating that at high concentrations it prevents subunit dissociation. At 50 μM Fru-1,6-P_2 (Fig. 7A, lane 4) the 1:3 and 3:1 hybrids begin to disappear, and at 500 μM (lane 6) the bands for the 2:2 hybrids were greatly weakened. In contrast, inhibitory concentrations of Fru-2,6-P_2 did not prevent the subunit exchange (Fig. 7B), and 200 mM KCl (Fig. 7C) did not alter the distribution either, in spite of the fact that it induces a conformational change. These results suggest that the conformational changes induced by Fru-2,6-P_2 and high

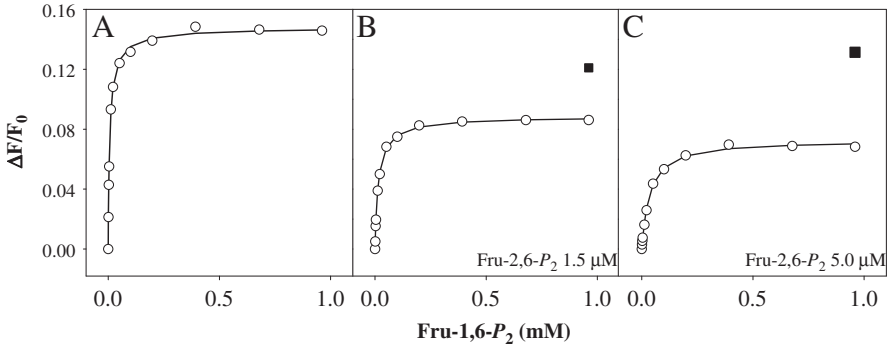

Fig. 6. Effect of the presence of Fru-2,6-P_2 on the fluorescence emission changes generated by Fru-1,6-P_2 binding to Phe219Trp FBPase. The sample of the enzyme (60 μg/ml in Tris/HCl pH 7.5 containing 0.1 mM EDTA) was titrated with substrate in the absence or in the presence of Fru-2,6-P_2. The fluorescence emission of the samples were measured before (F_0) and after the addition of Fru-2,6-P_2 (F_i) if this ligand was added. Panel A: $\Delta F = F - F_0$, where F is the observed fluorescence at a given concentration of substrate. Panels B and C: $\Delta F = F - F_i$. The points marked as ■ correspond to the values of $\Delta F/F_0$ at 1000 μM Fru-1,6-P_2, calculated using $\Delta F = F - F_0$. More details in Materials and methods.

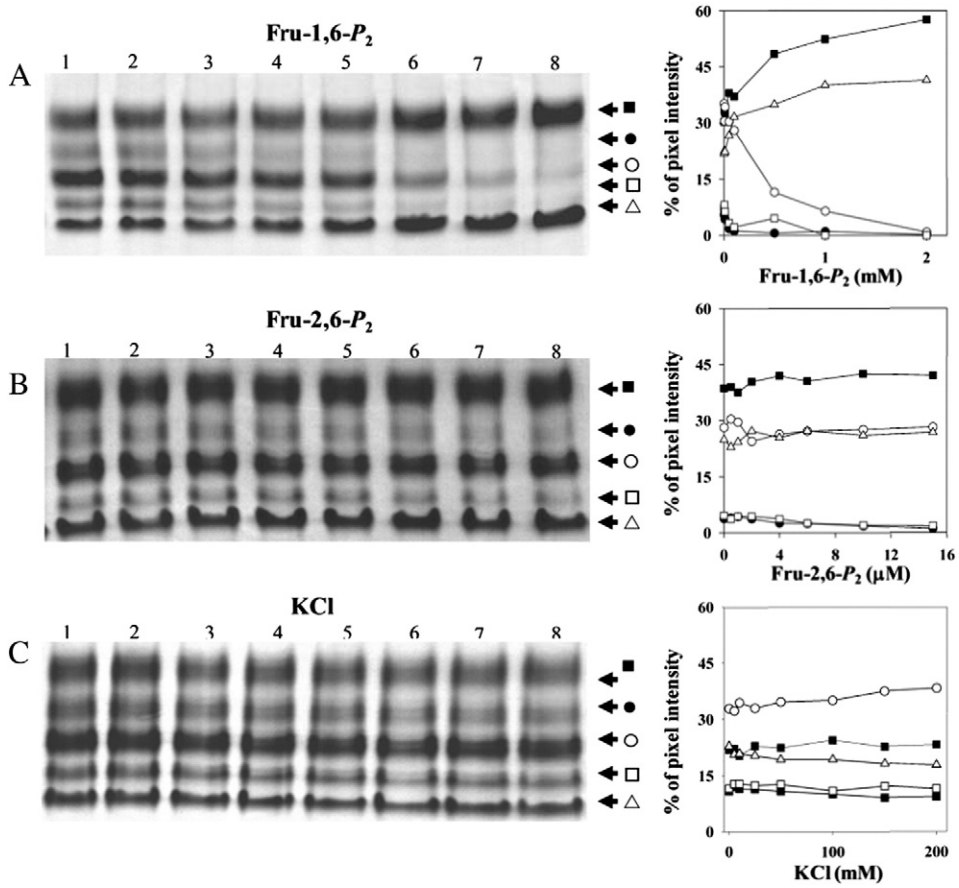

Fig. 7. Effect of fructose bisphosphates on the subunit exchange between wild-type and Glu-tagged fructose bisphosphatases as seen by 6% non-denaturing PAGE. The enzymes were mixed for hybridization in the presence of A: Fru-1,6-P_2 0; 5; 10; 50; 100; 500; 1000 and 2000 μM (lanes 1 to 8); B: Fru-2,6-P_2 0; 0,5; 1; 2; 4; 6; 10 and 15 μM (lanes 1 to 8) and C: 0; 5; 10; 25; 50; 100; 150 and 200 mM KCl, as a control for ionic strength (lanes 1 to 8). The bands corresponding to the different enzymes or hybrids with wild type: mutant subunit ratios of 4:0; 3:1; 2:2; 1:3 and 0:4, from top to bottom, are marked with arrows. The graphs on the right hand side of each gel were obtained with GeneSnap 7.4 software (Syngene) by density scans, the hybrids are represented by the following symbols: (■) 4:0; (●) 3:1; (○) 2:2; (□) 1:3 and (△) 0:4.

concentrations of Fru-1,6-P_2 are different, and that Fru-2,6-P_2 binds to the high-affinity sites and cannot induce the conformational change responsible for the low-affinity sites.

3.6. Susceptibility to substrate inhibition of FBPase hybrids containing subunits mutated at the active site

Tyr244 is located at the active site and is involved in the interaction of the 6-phospho group of Fru-1,6-P_2 [24,42,47]. A mixture of FBPase hybrids was obtained by subunit exchange between Glu-tagged homotetramer and Tyr244Phe FBPase, and the hybrids were separated on a Q-Sepharose column using a linear NaCl gradient (Fig. 8). The elution profile shows seven peaks, the first of which is devoid of enzymatic activity (Fig. 8A). The identity of each active peak was established by non-denaturing PAGE (Fig. 8B). As expected, the retention time increased with the numbers of Glu-tagged subunits in the tetramer. The first active peak (4:0) corresponds to Tyr244Phe FBPase and the last (0:4) to the Glu-tagged homotetramer. The second and penultimate active peaks correspond to the 3:1 hybrid (3 Tyr244Phe subunits to 1 Glu-tagged subunit) and to the 1:3 hybrid (1 Tyr244Phe subunit to 3 Glu-tagged subunits), respectively. The three different 2:2 hybrids were resolved into two peaks, the third active peak, assigned as a mixture of 2:2q and 2:2r hybrids and labeled 2:2qr, and the fourth active peak, assigned as 2:2p hybrid. These assignments were based on the fact that subunit exchange in the presence of Fru-1,6-P_2 occurs only in the hybrid with like subunits at positions C1C2 and corresponds in retention time to the 2:2p hybrid (fourth active peak) from the elution profile obtained without Fru-1,6-P_2 [35]. Hence the peak with retention time of about 198 min in the elution profile (Fig. 8A) corresponds to the 2:2p hybrid. The letters p, q and r refer to 2:2 hybrids with like subunits at positions C1C2, C1C4 and C2C4 of the tetramer, respectively [35]. The labels should have been pp, pq and pr respectively, as they refer to *pairs* of subunits as described by Cornish-Bowden and Koshland [48]. However, here we retain the symbols of ref. [35].

The substrate saturation curve of the Glu-tagged homotetramer exhibits the characteristic partial inhibition by substrate, whereas the Tyr244Phe homotetramer shows, as expected, both a decreased catalytic activity and a shift of the inhibition curve to higher substrate concentrations (Fig. 9A). In the range of 1.0–10 μM Fru-1,6-P_2 the 1:3 and 2:2p hybrids display similar rates to those for the Glu-tagged homotetramer; by contrast, the rates in this concentration range are smaller for the 2:2q/2:2r and 3:1 hybrids. Fig. 9B shows a comparison of the rates measured at 10 μM substrate. Only tetramers containing a dimer C1C2 or C3C4 with intact active sites have normal catalytic activity at non-inhibitory substrate concentrations. Thus the k_{cat} values of the 1:3 (15.9 s^{-1}) and 2:2p hybrids (18.0 s^{-1}) are similar to the k_{cat} value of 17.2 s^{-1} for the Glu-tagged FBPase, whereas the k_{cat} values of the 2:2q/2:2r (9.8 s^{-1}) and 3:1 hybrids (9.5 s^{-1}) are lower, close to that for the Tyr244Phe enzyme (7.1 s^{-1}). The K_m values for all the hybrids range from 9.6 to 16.5 μM, which are comparable with those of the wild-type and Glu-tagged FBPases. On the other hand, at substrate concentrations above 10 μM the rates observed for the 1:3 and 2:2p hybrids are higher than those measured for Glu-tagged FBPase, indicating shifts in the curves for substrate inhibition to higher concentrations. Fig. 9C

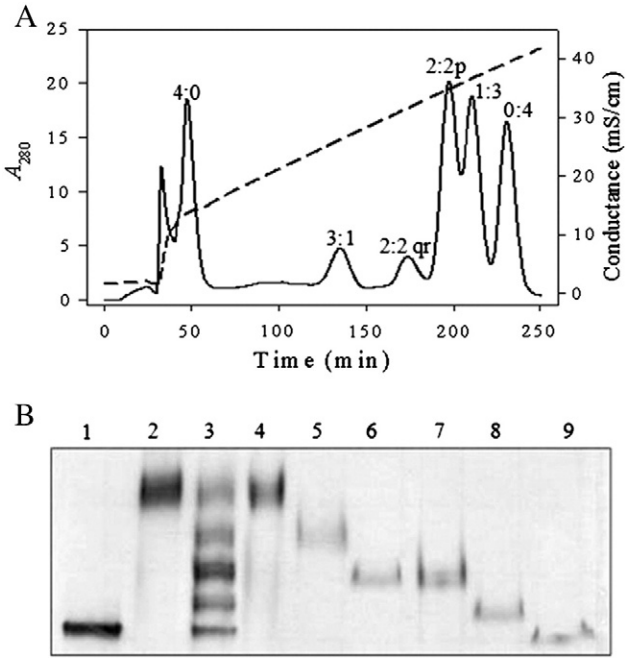

Fig. 8. Separation of hybrid FBPases by chromatography on Q-Sepharose. A: Elution profile of the hybrid mixture. The peaks with enzymatic activity are marked with letters. B: Non-denaturing PAGE of the purified hybrids. Lane 1, independently purified Glu-tagged FBPase; lane 2, independently purified Tyr244Phe FBPase; lane 3, hybrid mixture applied on the column; lane 4, peak 4:0 (Tyr244Phe FBPase); lane 5, peak 3:1 (the 3:1 hybrid); lane 6, peak 2:2q/r (mixture of 2:2q and 2:2r hybrids); lane 7, peak 2:2p; lane 8, peak 1:3; lane 9, peak 0:4 (Glu-tagged FBPase).

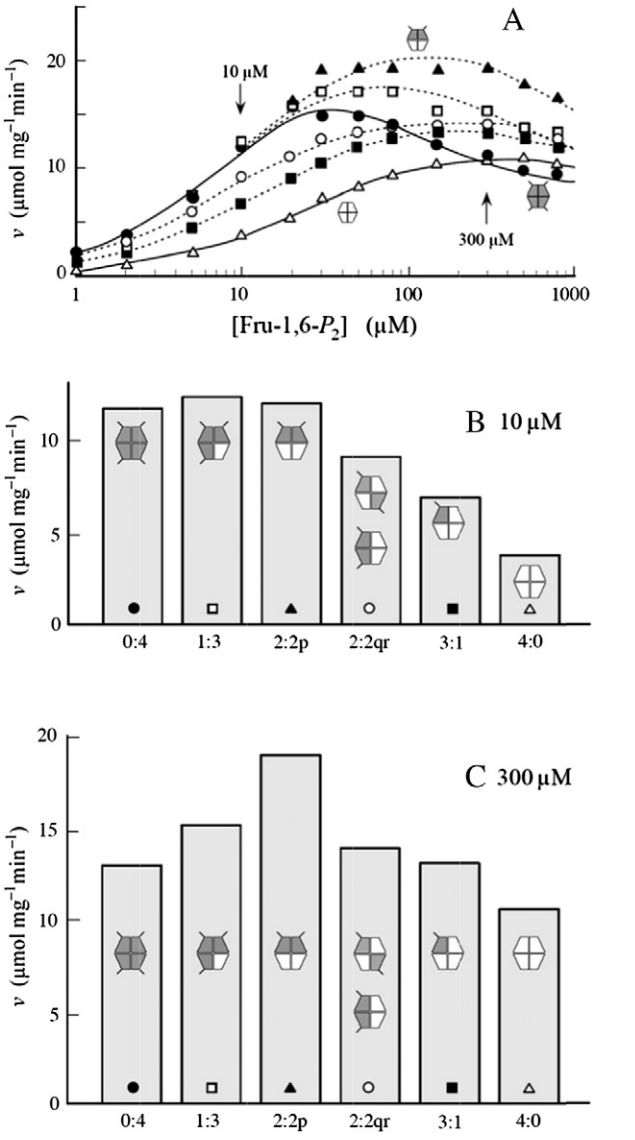

Fig. 9. Dependence of the enzymatic activity of Glu-tagged, Tyr244Phe and hybrid FBPases on the concentration of Fru-1,6-P_2. The samples were assayed immediately after isolation of the enzymes, which are represented by the following symbols: (●) Glu-tagged FBPase; (□) 1:3 hybrid; (▲) 2:2p hybrid; (○) 2:2q/2:2r hybrids; (■) 3:1 hybrid; (Δ) Tyr244Phe FBPase. Panel A shows rates as a function of the substrate concentration, ranging from 0.5 μM to 1.0 mM. Panels B and C show the rates obtained for the different tetramers at 10 μM (B) and 300 μM (C) substrate, as indicated by the arrows in panel A.

shows a comparison of the rates measured at 300 μM substrate. Strikingly, the 2:2p hybrid (with two intact active sites in the same dimer) has a much higher activity than the 2:2qr hybrids (again with two intact active sites, but now in different dimers): this implies that the two high-affinity sites are in the same dimer. Notice that a consequence of the higher substrate concentrations needed for inhibition is that the highest rate for the 2:2p hybrid is much higher than that for the Glu-tagged enzyme, and somewhat higher than for the 1:3 hybrid. Furthermore, although the Glu-tagged and Tyr244Phe FBPases show similar rates at 300 μM substrate (Fig. 9C), the latter requires a much higher substrate concentration to be inhibited (Fig. 9A).

4. Discussion

An earlier interpretation of inhibition of human muscle FBPase by excess substrate was made in terms of uncompetitive inhibition [13]. Rakus et al. [49] later investigated FBPases from pig and cattle lung (liver-like isozyme), and proposed a mechanism in terms of partial non-competitive inhibition that fitted well with the experimental data. They postulated that FBPase consists of two classes of the substrate binding site: the first catalytic and the second inhibitory. Our results with the pig kidney enzyme can be considered to extend and amplify this work. They indicate that the substrate inhibition of FBPase is due to subunit interactions, such that binding of the first Fru-1,6-P_2 molecule, in one dimer, induce lower affinity and catalytic activity of the two binding sites in the other dimer. Binding of Fru-2,6-P_2, on the other hand, appears not to induce the conformational change responsible for the appearance of the low-affinity sites, as it does not prevent the exchange of subunits that is suppressed by inhibitory concentrations of Fru-1,6-P_2. Nonetheless, the fluorescence measurements indicate that it does induce a conformational change, albeit not the same one.

Distinguishing between the two models of the dependence of the rate on the substrate concentration – one with the binding sites treated as four non-independent sites (Eq. (1)), the other with two pairs of two sites, each pair behaving independently of the other (Eq. (2)) – requires abundant and precise data over a wide range of concentrations, and this probably explains why the problem has remained unresolved. The K_m and k_{cat} values of FBPases have usually been determined using a modified form of the Michaelis–Menten equation that incorporates a term for substrate inhibition [33,34,49], which is of a similar type as Eq. (2). Although Eq. (2) gives an approximate account of the data, the *F* test for lack of fit provides arguments for rejecting the underlying model. Fitting the kinetic data of the substrate saturation curve to Eq. (1), for four non-independent sites, showed the existence of two binding sites of high and similar affinity (dissociation constants about 14 μM) and two binding sites of much lower affinity (dissociation constants about 390 μM). Binding of the second, third and fourth substrate molecules decrease the catalytic activity, with the greatest decrease occurring when the third molecule binds. The dissociation constant of the high-affinity sites agrees well with the value obtained by fluorometric titration. According to our results, binding of substrate at the low-affinity sites does not affect the emission of Trp219, as concentrations higher than 0.1 mM do not cause any further change. Furthermore, substrate

at inhibitory concentrations (>50 μM), but not at lower concentrations, prevents subunit exchange between native and Glu-tagged FBPase.

The conservative mutations Phe219Trp and Phe232Trp produce only minor changes in the functional properties of FBPase, so these tryptophan residues are non-perturbing spectroscopic probes of the enzyme conformation. Residue 219 is near the active site, positioned at the extreme of the loop L10, which contains residues Asn212 and Tyr215, which are postulated to make hydrogen bonds with the substrate and the inhibitor Fru-2,6-P_2 [11,41]. The Phe219Trp mutant senses the binding of the substrate and of Fru-2,6-P_2 by an increase in fluorescence. Residue 232, on the other hand, is situated at the end of the helix H6, near the C1–C2 interface [21], and the fluorescence emission of the Phe232Trp mutant was almost unaffected by the binding of the ligands Fru-1,6-P_2, Fru-2,6-P_2 and AMP, consistent with the high degree of exposure shown by the Stern–Volmer collisional quenching constant. The monophasic binding curve obtained by titration of Phe219Trp FBPase with substrate (Fig. 5A) is consistent with tight binding (dissociation constant about 8 μM) of a single molecule of the ligand to the tetrameric enzyme, or alternatively, the binding of two molecules of the ligand to sites of similar affinity.

The active sites in free FBPase appear to be identical, but become non-identical after a conformational change induced by binding of substrate to the first subunit, which results in the lower affinity of two of the other three subunits. The identity of the subunit to which the first substrate molecule binds probably determines the subunit to which the second binds. There could thus be a specific localization of high-affinity sites, either on the same dimer, at C1 and C2, or on different dimers at C1 and C3, or alternatively at C1 and C4. Comparison of substrate saturation curves of hybrid tetramers containing two subunits of normal activity together with two with decreased activity (Fig. 9), both with one another (2:2p compared with 2:2qr) and with the homotetrameric enzymes (2:2p compared with 0:4 and 4:0), indicates that the high-affinity substrate binding sites are on one dimer and the low-affinity sites on the other. This conclusion is supported by the fact that the 2:2p hybrid has almost the same catalytic activity as the Glu-tagged enzyme at noninhibitory substrate concentrations (0.5–10 μM) while the catalytic activity of the mixture of 2:2q and 2:2r hybrids is considerably lower, explained by the presence of a subunit with a mutated active site in each dimer. As expected, the substrate inhibition of the 2:2p hybrid is less than that of the Glu-tagged tetramer, as the mutation produces decreased affinity of the active sites available for the third and fourth substrate molecules. Thus binding of the first substrate molecule to a dimer of the enzyme (for instance C1C2) produces a conformational change at the other dimer (C3C4), reducing the affinity of its subunits for the substrate. This accords well with results of Nelson et al. [35], who showed that FBPase hybrids containing two subunits with functional AMP binding sites exhibit cooperative AMP inhibition if the functional subunits are on different dimers. It can be concluded that in both AMP and substrate inhibition, binding of the ligand to one subunit of a dimer elicits an affinity change of the binding sites on the subunits of the other dimer.

According to the calculated rate constants shown in Fig. 3A for Eq. (1) (Fig. 3B) binding of the first substrate molecule has almost no effect on the affinity of the enzyme for the second, but it produces an approximate halving of the rate. These results can be attributed to the communication between the active sites of monomer C1 and C2; it is conceivable that if two substrate molecules are bound simultaneously to a dimer, the presence of the substrate molecule in each site causes a reorientation of catalytic residues and/or the displacement of a catalytic metal ion at the adjacent active site. In this regard, crystallographic studies [42] have shown the interaction between helix H4 (residues 123–127) from one monomer (C1) and residues Tyr258 and Arg243 from the adjacent monomer (C2). Interestingly, Asp118 and Asp121 are catalytic residues located in a negatively charged pocket that binds divalent metal cations [50] and mutating them to Ala greatly diminishes catalytic activity of human liver FBPase [51]. The third and fourth substrate molecules then bind much more weakly than the first two, but with further changes in rate. It is important also to realize that the highest rate visible in Fig. 4 (about 20 μmol min^{-1} mg^{-1}) does not correspond to the value of V (37.6 μmol min^{-1} mg^{-1}), because at the concentration corresponding to this maximum there are substantial effects of substrate inhibition due to occupation of the second and later sites.

Our model extends previous studies of the mechanism of action of FBPase [13,49] in a number of ways. First of all, it accounts for the effects of Fru-1,6-P_2 over a very wide range of concentrations. Secondly, it recognizes that in the free enzyme the four active sites are identical, but that differences are induced by substrate binding, and finally it clarifies the importance of the structure of the enzyme as a dimer of dimers, so that binding of ligands in one dimer affects other binding sites differently according whether they are in the same dimer or not.

As the crystal structure of the enzyme was determined in the presence of high substrate or product (Fru-6-*P*; *P*i) concentrations [41,50,52] the kinetic results that we report imply that mechanisms based on the crystal structure inevitably refer to saturation of the low-affinity sites, and thus not to the enzyme in its most active state.

The mechanism that we propose for the substrate inhibition of FBPase recalls one that has been proposed for PFK-1 of *Escherichia coli*, which shows substrate inhibition by MgATP at low concentrations of Fru-6-*P*: Berger and Evans [53] suggested that MgATP binds at a second binding site distant from the active site, causing allosteric inhibition in the active site. However, Fenton and Reinhart [54] demonstrated that a hybrid tetramer of this enzyme with only one functional active site does not show substrate inhibition, highlighting the importance of intersubunit interactions for the regulatory mechanism of this enzyme. They proposed that MgATP in one active site behaves as an allosteric inhibitor of Fru-6-*P* affinity in a second active site, eliminating the need for a new MgATP binding site. If this sort of mechanism applies also to FBPase, as our results suggest, then the inhibition by excess substrate may be closely related to the inhibition by Fru-2,6-P_2, with the two molecules binding to the same site, but with different determinants. Then the inhibition by excess substrate at high concentrations can be seen as the price to be paid for the physiologically useful inhibition by Fru-2,6-P_2, which functions as a glycolytic signal over a wide range of plants, fungi, animals and protozoans [55]. That in turn would explain the evolutionary conservation of the substrate inhibition by Fru-1,6-P_2: even if the substrate inhibition on its own appears puzzling from a physiological point of view, it makes sense if it is regarded as a side effect of properties with a more obvious function.

Gluconeogenesis and glycogenolysis are pathways for glucose production, whereas glycolysis and glycogenesis are pathways for glucose utilization and storage. At the biochemical and molecular level, the metabolic and regulatory enzymes integrate hormonal and nutritional signals and regulate glucose flux in the liver. Modulating either activities or gene expression of these metabolic enzymes can control hepatic glucose production. Mimics of the substrate inhibition of FBPase may thus provide a future option for combatting both postprandial and fasting hyperglycemia.

Acknowledgements

J.L.A. and C.A.D. were recipients of doctoral fellowships granted by MECESUP-Chile AUS0006 and CONICYT-Chile AT/403167, respectively. This work was supported by grants 1090740 and 1141033 from FONDECYT (Chile) to J.C.S. and the Dirección de Investigación de la Universidad Austral de Chile. A.C.-B. and M.L.C. were supported by the CNRS, and the visit of A.C.-B. to Valdivia by FONDECYT 1090740 (International cooperation).

References

[1] H.G. Hers, L. Hue, Gluconeogenesis and related aspects of glycolysis, Annu. Rev. Biochem. 52 (1983) 617–653.

[2] G.A. Tejwani, Regulation of fructose-bisphosphatase activity, Adv. Enzymol. Relat. Areas Mol. Biol. 54 (1983) 121–194.
[3] E. Van Schaftingen, Fructose 2,6-bisphosphate, Adv. Enzymol. Relat. Areas Mol. Biol. 59 (1987) 315–395.
[4] S.J. Pilkis, T.H. Claus, Hepatic gluconeogenesis/glycolysis: regulation and structure/function relationships of substrate cycle enzymes, Annu. Rev. Nutr. 11 (1991) 465–515.
[5] A. Dzugaj, Localization and regulation of muscle fructose-1,6-bisphosphatase, the key enzyme of glyconeogenesis, Adv. Enzym. Regul. 46 (2006) 51–71.
[6] Ch. Wu, S.A. Khan, L.-J. Peng, A.J. Lange, Roles for fructose-2,6-bisphosphate in the control of fuel metabolism: beyond its allosteric effects on glycolytic and gluconeogenic enzymes, Adv. Enzym. Regul. 46 (2006) 72–88.
[7] J.K. Hines, X. Chen, J.C. Nix, H.J. Fromm, R.B. Honzatko, Structures of mammalian and bacterial fructose-1,6-bisphosphatases reveal the basis for synergism in AMP/fructose-2,6-bisphosphate inhibition, J. Biol. Chem. 282 (2007) 36121–36131.
[8] K. Taketa, B.M. Pogell, Allosteric inhibition of rat liver fructose 1,6-diphosphatase by adenosine 5′-monophosphate, J. Biol. Chem. 240 (1965) 651–662.
[9] F. Liu, H.J. Fromm, Relationship between thiol group modification and the binding site for fructose 2,6-bisphosphate on rabbit liver fructose-1,6-bisphosphatase, J. Biol. Chem. 263 (1988) 10035–10039.
[10] A.M. Reyes, E. Hubert, J.C. Slebe, The reactive cysteine residue of pig kidney fructose 1,6-bisphosphatase is related to a fructose 2,6-bisphosphate allosteric site, Biochem. Biophys. Res. Commun. 127 (1985) 373–379.
[11] J.Y. Liang, S. Huang, Y.P. Zhang, H.M. Ke, W.N. Lipscomb, Crystal structure of the neutral form of fructose 1,6-bisphosphatase complexed with regulatory inhibitor fructose 2,6-bisphosphate at 2.6-A resolution, Proc. Natl. Acad. Sci. U. S. A. 89 (1992) 2404–2408.
[12] A.M. Reyes, N. Bravo, H.C. Ludwig, A. Iriarte, J.C. Slebe, Modification of Cys-128 of pig kidney fructose 1,6-bisphosphatase with different thiol reagents: size dependent effect on the substrate and fructose-2,6-bisphosphate interaction, J. Protein Chem. 12 (1993) 159–168.
[13] K. Skalecki, W. Mularczyk, A. Dzugaj, Kinetic properties of D-fructose-1, 6-bisphosphate 1-phosphohydrolase isolated from human muscle, Biochem. J. 310 (1995) 1029–1035.
[14] R.J. Hodgson, Z. Jia, W.C. Plaxton, A fluorescence study of ligand-induced conformational changes in cytosolic fructose-1,6-bisphosphatase from germinating castor oil seeds, Biochim. Biophys. Acta 1388 (1998) 285–294.
[15] L. Garcia-Rejón, M.J. Sanchez-Muros, J. Cerdá, M. de la Higuera, Fructose-1,6-bisphosphatase activity in liver and gonads of sea bass (*Dicentrarchus labrax*). Influence of diet composition and stage of the reproductive cycle, Fish Physiol. Biochem. 16 (1997) 93–105.
[16] J.J. Aragón, V. Sánchez, L. Boto, Fructose-2,6-bisphosphate in *Dictyostelium discoideum*. Independence of cyclic AMP production and inhibition of fructose-1, 6-bisphosphatase, Eur. J. Biochem. 161 (1986) 757–761.
[17] G.M. Lloyd, Kinetic properties of phosphofructokinase (and fructose-1, 6-bisphosphatase) of the liver fluke *Fasciola hepatica*, Int. J. Parasitol. 13 (1983) 475–481.
[18] C.H. Verhees, J. Akerboom, E. Schlitz, M. de Vos, J. van der Oost, Molecular and biochemical characterization of a distinct type of fructose-1,6-bisphosphatase from *Pyrococcus furiosus*, J. Bacteriol. 184 (2002) 3401–3405.
[19] J. Babul, V. Guixe, Fructose-1,6-bisphosphatase from *Escherichia coli*. Purification and characterization,, Arch. Biochem. Biophys. 225 (1983) 944–949.
[20] P.F. Cook, W.W. Cleland, Enzyme Kinetics and Mechanism, Garland Science, London and New York, 2007. 173–181.
[21] Y. Zhang, J.Y. Liang, S. Huang, W.N. Lipscomb, Toward a mechanism for the allosteric transition of pig kidney fructose-1,6-bisphosphatase, J. Mol. Biol. 244 (1994) 609–624.
[22] H.C. Ludwig, F.N. Pardo, J.L. Asenjo, M.A. Maureira, A.J. Yáñez, J.C. Slebe, Unraveling multistate unfolding of pig kidney fructose-1,6-bisphosphatase using single tryptophan mutants, FEBS J. 274 (2007) 5337–5349.
[23] H.M. Ke, Y.P. Zhang, W.N. Lipscomb, Crystal structure of fructose-1,6-bisphosphatase complexed with fructose 6-phosphate, AMP, and magnesium, Proc. Natl. Acad. Sci. U. S. A. 87 (1990) 5243–5247.
[24] H.M. Ke, J.Y. Liang, Y.P. Zhang, W.N. Lipscomb, Conformational transition of fructose-1,6-bisphosphatase: structure comparison between the AMP complex (T form) and the fructose 6-phosphate complex (R form), Biochemistry 30 (1991) 4412–4420.
[25] S.W. Wright, A.A. Carlo, M.D. Carty, D.E. Danley, D.L. Hageman, G.A. Karam, C.B. Levy, M.N. Mansour, A.M. Mathiowetz, L.D. McClure, N.B. Nestor, R.K. McPherson, J. Pandit, L.R. Pustilnik, G.K. Schulte, W.C. Soeller, J.L. Treadway, I.-K. Wang, P.H. Bauer, Anilinoquinazoline inhibitors of fructose 1,6-bisphosphatase bind at a novel allosteric site: synthesis, *in vitro* characterization, and X-ray crystallography, J. Med. Chem. 45 (2002) 3865–3877.
[26] J.-Y. Choe, S.W. Nelson, K.L. Arienti, F.U. Axe, T.L. Collins, T.K. Jones, R.D.A. Kimmich, M.J. Newman, K. Norvell, W.C. Ripka, S.J. Romano, K.M. Short, D.H. Slee, H.J. Fromm, R.B. Honzatko, Inhibition of fructose-1,6-bisphosphatase by a new class of allosteric effectors, J. Biol. Chem. 278 (2003) 51176–51183.
[27] M.D. Erion, Q. Dang, M.R. Reddy, S.R. Kasibhatla, J. Huang, W.N. Lipscomb, P.D. van Poelje, Structure-guide design of AMP mimics that inhibit fructose-1,6-bisphosphatase with high affinity and specificity, J. Am. Chem. Soc. 129 (2007) 15480–15490.
[28] S. Heng, K.R. Gryncel, E.R. Kantrowitz, A library of novel allosteric inhibitors against fructose 1,6-bisphosphatase, Bioorg. Med. Chem. 17 (2009) 3916–3922.
[29] Q. Dang, Y. Liu, D.K. Cashion, S.R. Kasibhatla, T. Jiang, F. Taplin, J.D. Jacintho, H. Li, Z. Sun, Y. Fan, J. DaRe, F. Tian, W. Li, T. Gibson, R. Lemus, P.D. van Poelje, S.C. Potter, M.D. Erion, Discovery of a series of phosphonic acid-containing thiazoles and orally bioavailable diamide prodrugs that lower glucose in diabetic animals through inhibition of fructose-1,6-bisphosphatase, J. Med. Chem. 54 (2011) 153–165.
[30] P.D. van Poelje, S.C. Potter, V.C. Chandramouli, B.R. Landau, Q. Dang, M.D. Erion, Inhibition of fructose 1,6-bisphosphatase reduces excessive endogenous glucose production and attenuates hyperglycemia in Zucker diabetic fatty rats, Diabetes 55 (2006) 1747–1754.
[31] T. Yoshida, A. Okuno, K. Takahashi, J. Ogawa, Y. Hagisawa, S. Kanda, T. Fujiwara, Contributions of hepatic gluconeogenesis suppression and compensative glycogenolysis on the glucose-lowering effect of CS-917, a fructose 1,6-bisphosphatase inhibitor, in non-obese type 2 diabetes Goto-Kakizaki rats, J. Pharmacol. Sci. 115 (2011) 329–335.
[32] R. Bertinat, J.P. Pontigo, M. Pérez, I.I. Concha, R.S. Martín, J.J. Guinovart, J.C. Slebe, A.J. Yáñez, Nuclear accumulation of fructose 1,6-bisphosphatase is impaired in diabetic rat liver, J. Cell. Biochem. 113 (2012) 848–856.
[33] J.G. Cárcamo, A.J. Yáñez, H.C. Ludwig, O. León, R.O. Pinto, A.M. Reyes, J.C. Slebe, The C1–C2 interface residue lysine 50 of pig kidney fructose-1, 6-bisphosphatase has a crucial role in the cooperative signal transmission of the AMP inhibition, Eur. J. Biochem. 267 (2000) 2242–2251.
[34] G. Lu, M.K. Williams, E.L. Giroux, E.R. Kantrowitz, Fructose-1,6-bisphosphatase: arginine-22 is involved in stabilization of the T allosteric state, Biochemistry 34 (1995) 13272–13277.
[35] S.W. Nelson, R.B. Honzatko, H.J. Fromm, Hybrid tetramers of porcine liver fructose-1,6-bisphosphatase reveal multiple pathways of allosteric inhibition, J. Biol. Chem. 277 (2002) 15539–15545.
[36] U.K. Laemmli, Cleavage of structural proteins during the assembly of the head of bacteriophage T4, Nature 227 (1970) 680–685.
[37] A. Cornish-Bowden, L. Endrenyi, Fitting of enzyme kinetic data without prior knowledge of weights, Biochem. J. 193 (1981) 1005–1008.
[38] A. Cornish-Bowden, Analysis of Enzyme Kinetic Data, Oxford University Press, 1995.
[39] N.R. Draper, H. Smith, Applied Regression Analysis, 2nd edn Wiley–Interscience, 1981.
[40] N. Kelley-Loughnane, E.R. Kantrowitz, AMP inhibition of pig kidney fructose-1,6-bisphosphatase, Biochim. Biophys. Acta 1548 (2001) 66–71.
[41] Y.P. Zhang, J.Y. Liang, S. Huang, H.M. Ke, W.N. Lipscomb, Crystallographic studies of the catalytic mechanism of the neutral form of fructose-1,6-bisphosphatase, Biochemistry 32 (1993) 1844–1857.
[42] Y. Xue, S. Huang, J.Y. Liang, Y. Zhang, W.N. Lipscomb, Crystal structure of fructose-1,6-bisphosphatase complexed with fructose 2,6-bisphosphate, AMP, and Zn^{2+} at 2.0-A resolution: aspects of synergism between inhibitors, Proc. Natl. Acad. Sci. U. S. A. 91 (1994) 12482–12486.
[43] J.Y. Liang, Y.P. Zhang, S. Huang, W.N. Lipscomb, Allosteric transition of fructose-1,6-bisphosphatase, Proc. Natl. Acad. Sci. U. S. A. 90 (1993) 2132–2136.
[44] J.R. Lakowicz, Principles of Fluorescence Spectroscopy, 2nd ed. Kluver Academic/Plenum Publishers, New York, 2006.
[45] C.A. Caperelli, W.A. Frey, S.J. Benkovic, Isotope-trapping experiments with rabbit liver fructose-1,6-bisphosphatase, Biochemistry 17 (1978) 1699–1704.
[46] S.J. Benkovic, M.M. deMaine, Mechanism of action of fructose-1,6-bisphosphatase, Adv. Enzymol. 53 (1982) 45–82.
[47] H. Ke, Y.P. Zhang, J.Y. Liang, W.N. Lipscomb, Crystal structure of neutral form of fructose-1,6-bisphosphatase complexed with the product fructose-6-phosphate at 2.1 Å resolution, Proc. Natl. Acad. Sci. U. S. A. 88 (1991) 2989–2993.
[48] A.J. Cornish-Bowden, D.E. Koshland Jr., The quaternary structure of proteins composed of identical subunits, J. Biol. Chem. 246 (1971) 3092–3102.
[49] D. Rakus, K. Skalecki, A. Dzugaj, Kinetic properties of pig (*Sus scrofa domestica*) and bovine (*Bos Taurus*) D-fructose-1,6-bisphosphate 1-phosphohydrolase (F1,6BPase). Liver-like isozymes in mammalian lung tissue, Comp. Biochem. Physiol. B 127 (2000) 123–134.
[50] J.-Y. Choe, S.W. Nelson, H.J. Fromm, R.B. Honzatko, Interaction of Tl^{+} with product complexes of fructose-1,6-bisphosphatase, J. Biol. Chem. 278 (2003) 16008–16014.
[51] M.R. El-Maghrabi, M. Gidh-Jain, L.R. Austin, S.J. Pilkis, Isolation of a human liver fructose-1,6-bisphosphatase cDNA and expression of the protein in *Escherichia coli.* Purification and characterization, J. Biol. Chem. 268 (1993) 9466–9472.
[52] J.-Y. Choe, H.J. Fromm, R.B. Honzatko, Crystal structures of fructose-1, 6-bisphosphatase: mechanism of catalysis and allosteric inhibition revealed in product complexes, Biochemistry 39 (2000) 8565–8574.
[53] S.A. Berger, P.R. Evans, Steady-state fluorescence of Escherichia coli phosphofructokinase reveals a regulatory role for ATP, Biochemistry 30 (1991) 8477–8480.
[54] A.W. Fenton, G.D. Reinhart, Mechanism of substrate inhibition in *Escherichia coli* phosphofructokinase, Biochemistry 42 (2003) 12676–12681.
[55] E. Van Schaftingen, E. Martens, F.R. Opperdoes, Fructose-2,6-bisphosphate in primitive systems, Fructose-2,6-bisphosphate, CRC Press, Boca Ratón, FL, 1990, pp. 229–244.